

REPORT DOCUMENTATION PAGE				Form Approved OMB No. 0704-0188	
<p>The public reporting burden for this collection of information is estimated to average 1 hour per response, including the time for reviewing instructions, searching existing data sources, gathering and maintaining the data needed, and completing and reviewing the collection of information. Send comments regarding this burden estimate or any other aspect of this collection of information, including suggestions for reducing the burden, to Department of Defense, Washington Headquarters Services, Directorate for Information Operations and Reports (0704-0188), 1215 Jefferson Davis Highway, Suite 1204, Arlington, VA 22202-4302. Respondents should be aware that notwithstanding any other provision of law, no person shall be subject to any penalty for failing to comply with a collection of information if it does not display a currently valid OMB control number.</p> <p>PLEASE DO NOT RETURN YOUR FORM TO THE ABOVE ADDRESS.</p>					
1. REPORT DATE (DD-MM-YYYY)		2. REPORT TYPE Conference Proceeding		3. DATES COVERED (From - To) 21-25 Oct 2002	
4. TITLE AND SUBTITLE Coupling GLERL with RAMS to Study Surface Wind Wave Effects on Air-Sea Fluxes in Chesapeake Bay				5a. CONTRACT NUMBER	
				5b. GRANT NUMBER N00014-98-1-0837	
				5c. PROGRAM ELEMENT NUMBER	
				5d. PROJECT NUMBER	
6. AUTHOR(S) Weiqi Lin, Lawrence Sanford, Jeff McQueens, Steven Suttles, Paul A. Hwang				5e. TASK NUMBER	
				5f. WORK UNIT NUMBER	
7. PERFORMING ORGANIZATION NAME(S) AND ADDRESS(ES) Naval Research Laboratory Oceanography Division Stennis Space Center, MS 39529-5004				8. PERFORMING ORGANIZATION REPORT NUMBER NRL/PP/7330/02/0092	
9. SPONSORING/MONITORING AGENCY NAME(S) AND ADDRESS(ES) Office of Naval Research 800 N. Quincy St. Arlington, VA 22217-5660				10. SPONSOR/MONITOR'S ACRONYM(S) ONR	
				11. SPONSOR/MONITOR'S REPORT NUMBER(S)	
12. DISTRIBUTION/AVAILABILITY STATEMENT Approved for public release; distribution is unlimited					
13. SUPPLEMENTARY NOTES					
14. ABSTRACT <p>Surface wind waves play an important role in the air-sea transfer of momentum, mass and heat. Several field experiments reported that wave age, C/u. (C_p is the wave phase velocity at spectral peak), is an important parameter for determining air-sea drag coefficient, C_d, or surface roughness length, Z_g (Donelan 1990; Geemaert et al. 1987; Smith et al. 1992; Lin 2000; Lin et al. 2002). Other theoretical or modeling studies (Janssen 1989, 1991) also suggested that wave age is a controlling factor for determining Z_g. Wave breaking generates air bubbles and significantly enhances gas transfer over water surface (Loewen 2002). Most recently, Deane and Stokes (2002) found that the size distribution of the entrained bubbles is critical to the way that air and sea interacts.</p>					
15. SUBJECT TERMS GLERL, RAMS, Chesapeake Bay <div style="text-align: center; font-size: 2em; font-weight: bold; margin-top: 10px;">20030523 101</div>					
16. SECURITY CLASSIFICATION OF:			17. LIMITATION OF ABSTRACT		18. NUMBER OF PAGES
a. REPORT Unclassified	b. ABSTRACT Unclassified	c. THIS PAGE Unclassified	SAR		11
			19a. NAME OF RESPONSIBLE PERSON Paul Hwang		
			19b. TELEPHONE NUMBER (Include area code) 228-688-4708		

COUPLING GLERL WITH RAMS TO STUDY SURFACE WIND WAVE EFFECTS ON AIR-SEA FLUXES IN CHESAPEAKE BAY

Weiqli Lin¹, Lawrence P. Sanford², Jeff McQueen³, Steven E. Suttles², and Paul A. Hwang¹

¹Oceanography Division, Naval Research Laboratory
Stennis Space Center, Mississippi 39529-5004, USA

²University of Maryland Center for Environmental Science
Horn Point Laboratory, Cambridge, Maryland 21613, USA

³Air Resource Laboratory, National Oceanic and Atmospheric Administration
Silver Spring, Maryland 20910, USA

1. INTRODUCTION

Surface wind waves play an important role in the air-sea transfer of momentum, mass and heat. Several field experiments reported that wave age, C_p/u . (C_p is the wave phase velocity at spectral peak), is an important parameter for determining air-sea drag coefficient, C_d , or surface roughness length, z_0 (Donelan 1990; Geernaert et al. 1987; Smith et al. 1992; Lin 2000; Lin et al. 2002). Other theoretical or modeling studies (Janssen 1989, 1991) also suggested that wave age is a controlling factor for determining z_0 . Wave breaking generates air bubbles and significantly enhances gas transfer over water surface (Loewen 2002). Most recently, Deane and Stokes (2002) found that the size distribution of the entrained bubbles is critical to the way that air and sea interacts.

Meso-scale meteorology models currently used to predict surface winds and air-sea fluxes do not include a sea state dependent surface roughness length over water surface. Fully coupling a wave model with a meteorology model seems to be the best way to address the surface wave effects on the air-sea fluxes of momentum, mass and heat. In a coupled wave/atmosphere modeling study, Doyle (1995) found that young wind seas significantly increase the surface wind stress. Desjardins et al. (2000) reported a 10% surface wind and 30% air-sea flux difference between the coupled and uncoupled model runs in the Atlantic Ocean Hurricanes. In the same study, Lalbeharry et al. (2000) found that the significant wave heights show better agreement with the buoy observations. These coupling studies were conducted in the open ocean where young wave seas are present occasionally but not dominated. In a shallow, (semi-) enclosed coastal environment, such as Chesapeake Bay (CB), fetch-limited young wind sea dominate the ocean surface wind waves, and the wave effects on the air-sea fluxes are expected to reach the maximum. The objective of this paper is to present a full coupled modeling study on wave effects on air-sea fluxes in the CB, an entirely fetch limited coastal environment with dominated young wind seas.

In summer 1998, a joint tower experiment was carried out by University of Maryland Center for Environmental Science (UMCES) Horn Point Laboratory (HPL), and Air Resources Laboratory (ARL), NOAA. A unique data set of air-sea fluxes and surface wind waves was collected in mid-CB from July 19-28, under low to moderate wind conditions. Lin et al. (2002) described the tower setup, data analysis, modeling results of the experiment. The analyzed data show that neutral drag coefficients depend upon both wind speed and wave age. They are better correlated to wave age than wind speed. Under light winds, the neutral drag coefficients increase with decreasing wind speed and have values much higher than those for relatively higher wind speeds. At higher wind speeds, neutral drag coefficients increase with increasing wind speed. Regardless of wind speed, neutral drag coefficients always decrease with increasing wave age. A parametric, deep water numerical wave model, Great Lakes Environmental Research Laboratory wave model (GLERL), developed by Donelan (1977) is modified to include a sea state dependent form drag and a reference system moving with the waves. It is used to study the wave effects on momentum transfer across the air water interface. The relationship between modeled drag coefficient and modeled wave age agreed well with the relationship derived from the data. GLERL model predicts total drag as a byproduct of the wave calculation and is computationally fast. It is shown to be a good tool for coupling with meso-scale atmospheric models to effect improved, fully coupled

Reproduced From
Best Available Copy

Copies Furnished to DTIC
Reproduced From
Bound Original

estimates of winds, waves, and air-sea fluxes of momentum and heat.

In this paper, we present a next-step study for the tower experiment. The GLERL was fully coupled with the Regional Atmosphere Modeling System (RAMS), a meso-scale meteorology model operationally used at ARL/NOAA. The sea state dependent over water sea surface roughness was fed back to the RAMS during the coupling processes. The GLERL predicted surface waves, RAMS predicted surface winds and heat fluxes were compared between the coupled/uncoupled runs and the data. It is found that fully coupled model runs can result in a significant difference between the GLERL predicted waves and RAMS predicted winds and heat fluxes. The surface wind waves play an important role in RAMS predictions of momentum and heat fluxes in the CB. The layout of the paper is as follows: In section 2, both GLERL and RAMS models are briefly described; The coupling procedure and results are presented in section 3; Summary and conclusion is given in section 4.

2. THE GLERL AND RAMS MODEL

2.1. The GLERL model

The GLERL wave model is a parametric, deep water numerical wave model. The model was developed by Donelan (1977) and used for wind wave forecasts in the Great Lakes (Schwab et al. 1984). Its basic equation is a local momentum balance equation. It is time dependent and can accommodate arbitrary wind and geography. Shallow water wave effects are not included, however. The wave energy spectrum $E(f)$ is assumed to follow the JONSWAP spectral shape (Hasselmann et al. 1973).

In the GLERL model, the total drag between air and water is treated as the sum of a skin friction (proportional to U_{n10}^2) and a form drag. The skin friction used in the model is defined as

$$\tau_s = \rho_a C_{d_s} U_{n10}^2, \quad (1)$$

where $C_{d_s}=0.7 \times 10^{-3}$ is the skin friction coefficient. The form drag of the wind over the waves, τ_f , is assumed to be proportional to the square of the relative velocity between wind velocity and wave phase velocity, such as

$$\tau_f = \rho_a D_f (U_{n10} - C) |U_{n10} - C|, \quad (2)$$

where C is wave phase velocity and D_f is the form drag coefficient given by

$$D_f = \left[\frac{\kappa}{\ln(10/z_0)} \right]^2. \quad (3)$$

The wave form drag changes with the development of waves, such that in a fully developed sea the dominant waves travel at phase speeds close to the driving wind velocity and τ_f becomes smaller and smaller. Full development corresponds to wave age, $C_p/U_{n10}=1.2$ (Donelan 1990). A relationship between the mean wave phase velocity, C , and peak wave phase velocity, C_p , was derived as $C_p/C=1.2$. Using this relationship

$$\tau_f = \rho_a D_f (U_{n10} - 0.83 C_p) \times |U_{n10} - 0.83 C_p|. \quad (4)$$

In the original model, $z_0 = \sigma/5$ was used where $\sigma^2 = \int_0^\infty E(f) df$ is the variance of surface elevation. We tested this expression against the data and found that it predicted values of z_0 that were one to two orders of magnitude higher than

the observed surface roughness. We modified the model to calculate z_0 using a formulation by Donelan (1990), which explicitly accounts for the effect of wave age on surface roughness and agrees better with the data. The formulation is given by

$$\frac{z_0}{H_s} = 1.38 \times 10^{-4} \left(\frac{C_p}{U_{n10}} \right)^{-2.66} \quad (5)$$

Finally, Cd is calculated as

$$Cd = \frac{\tau_f + \tau_s}{\rho_a U_{n10}^2} \quad (6)$$

Estimated Cd is output based on the driving wind speeds and predicted wave conditions at each hour.

2.2. The RAMS model

The RAMS is a meso-scale meteorology model developed at Colorado State University (Pielke et al. 1992). ARL/NOAA uses the RAMS to predict transport and dispersion from radioactive releases. The RAMS and the other meteorology models such as ETA and RSM are used at ARL to support air quality emergency response forecasting. The RAMS is also evaluated for air pollution deposition into the CB. McQueen et al. (1994, 1997) summarized RAMS applications to create a meso-scale, real-time meteorological forecasts of surface winds and air-sea fluxes over the CB.

During its operation, the RAMS was initialized from National Center for Environmental Prediction (NCEP) model fields such as ETA, AVN, and NGM. Many surface variables such as soil moisture, soil and vegetation type, canopy temperature and water content, terrain height, land roughness, land percentage and sea surface temperature are ingested into the RAMS on the model grid. The over water surface roughness is given by (Valigura 1995)

$$z_0 = \frac{0.016 u_*^2}{g} + \frac{K}{9.1 u_*} \quad (7)$$

where K is the molecular diffusivity of heat. The first term on the right hand side of Eq. (7) is the standard Charnock (1955) formulation with a constant of $\alpha = 0.016$, and the second term corrects for the increasing roughness at very low wind speeds. The z_0 in Eq. (7) depends only on wind speed. It is replaced by the GLERL model predicted z_0 to include a sea state dependent surface roughness length in the coupling process.

The RAMS determines turbulent fluxes of heat, H , and moisture, LH , over water via the standard bulk-transfer coefficient equations

$$H = \rho_a c_p D_H U_z (T_0 - T_z) \quad (8)$$

$$LH = \rho_a L_w D_w U_z (q_0 - q_z) \quad (9)$$

where T is temperature, q is specific heat, L_w is the latent heat of vaporization for water, c_p is the specific heat of air and

D_w, D_H are transfer coefficients of heat and water. These transfer coefficients are in turn functions of surface roughness and atmospheric boundary layer stability (McQueen et al. 1994).

2.3. The RAMS and GLERL modeling domain

The RAMS was run operationally over the CB with a finest mesh of 4 km and 25 vertical levels. The total number of grid points covering the RAMS grid were 82×102 . The area to be modeled was 296×376 km as shown in Fig. 1. The RAMS was run in both an assimilative and forecast mode.

The GLERL model domain is represented by horizontal grids, covering a rectangle domain. The modeled area was 128×308 km, which is in the RAMS grid (Fig. 1). The west-east direction was chosen as X direction with 321 grid points. The spatial spacing in X is equal to 400 m with a total length of 128 km. The south-north direction is chosen as Y direction with 771 grid points. The spatial spacing in Y is 400 m with a total length of 308 km.

A conformal Lambert Polar Conical projection (Taylor 1997) was used for the modeling domain. The latitude and longitude of the tangent point with both models was at (38.25, -76.5). The grid spacing was 4 km for RAMS and 400 m for GLERL, allowing RAMS grids to roughly match the GLERL grids every tenth grid. The central grids of RAMS was at (37, 47), matching the tangent point of (141, 401) in GLERL grids.

The GLERL was run in a UNIX system (DS20 DEC ALPHA) with 1,000 MHz EV6 CPU at HPL/UMCES. The execution time for one hour wind field ranged from one to several minutes, depending upon the maximum wind speed in the hour. The RAMS was run at an 8 processor (250 Mhz each) SGI Origin 2000 at ARL/NOAA. The output files from each model were transferred through the high speed network connection between HPL and ARL.

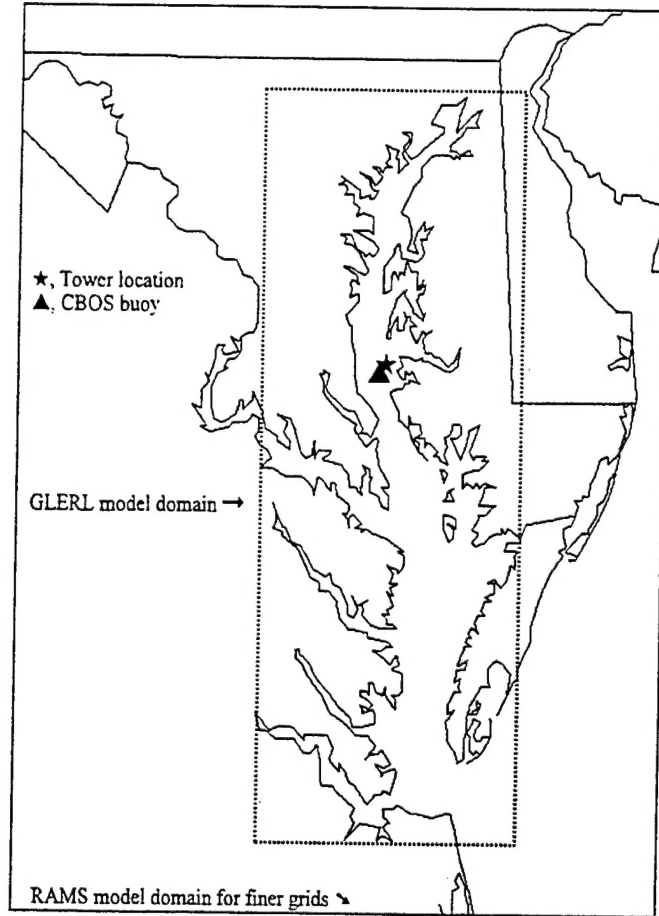


Fig. 1 The GLERL and RAMS (finer grids) model domain, and the tower and CBOS buoy location.

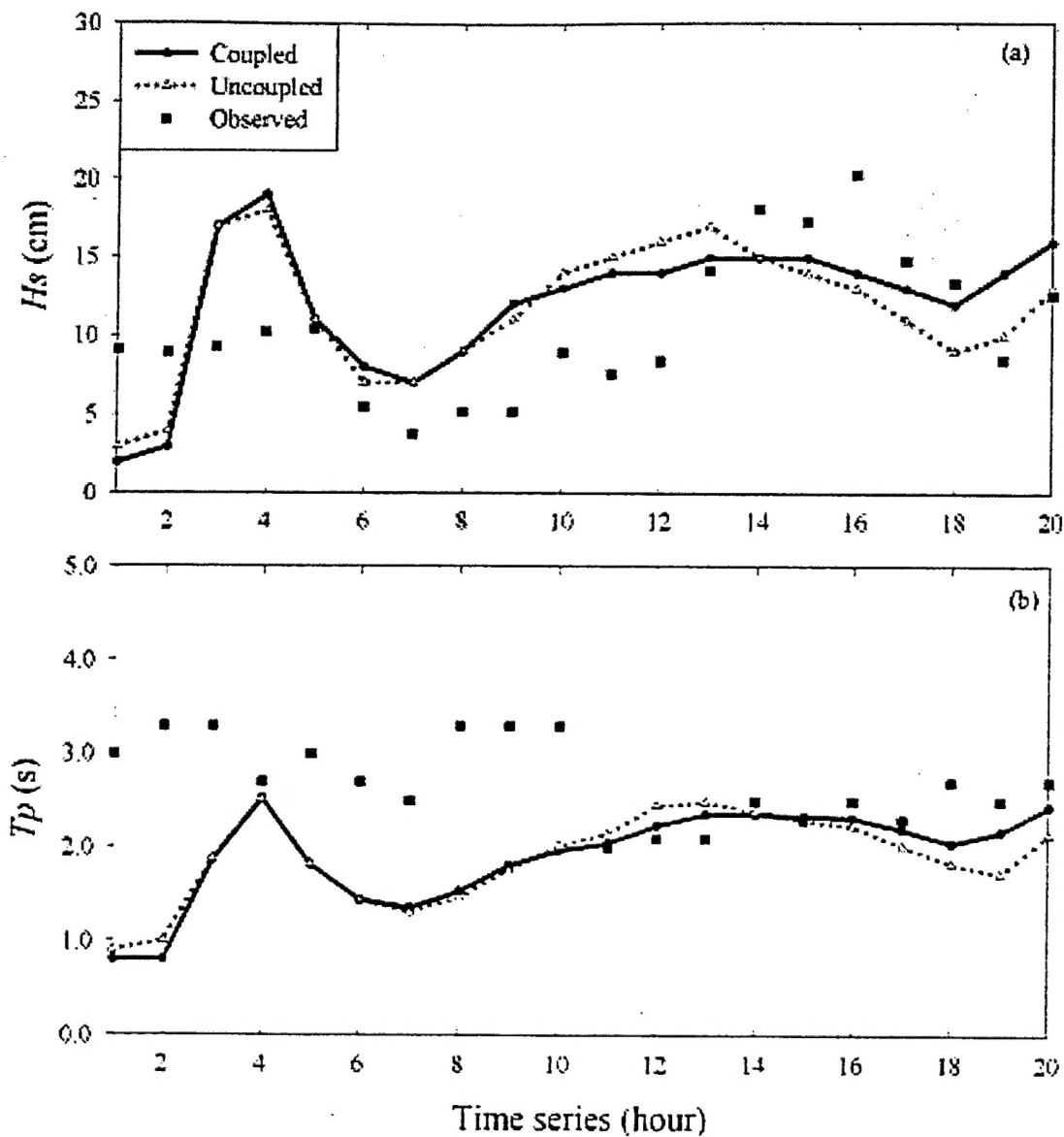


Fig. 2 A twenty hour time series of significant wave heights (a) and peak period (b) predicted by the coupled (solid line with open triangles) and uncoupled (dotted line with solid circles) GLERL model. The observed wave data at the tower location is shown by solid squares.

3. THE COUPLED MODEL RUNS AND RESULTS

3.1. The uncoupled model runs

Before the two models were coupled, the RAMS was run with a series of fourteen hour simulations. A two-day simulation was completed with a 4×14 hour simulation. The first two hour simulation was replaced by the last two hour simulation, reducing model spin-up of moisture which occurred during the first three hour of a model simulation.

Following the procedure below, the uncoupled RAMS was run from 1200 UTC July 22 to 1200 UTC July 24.

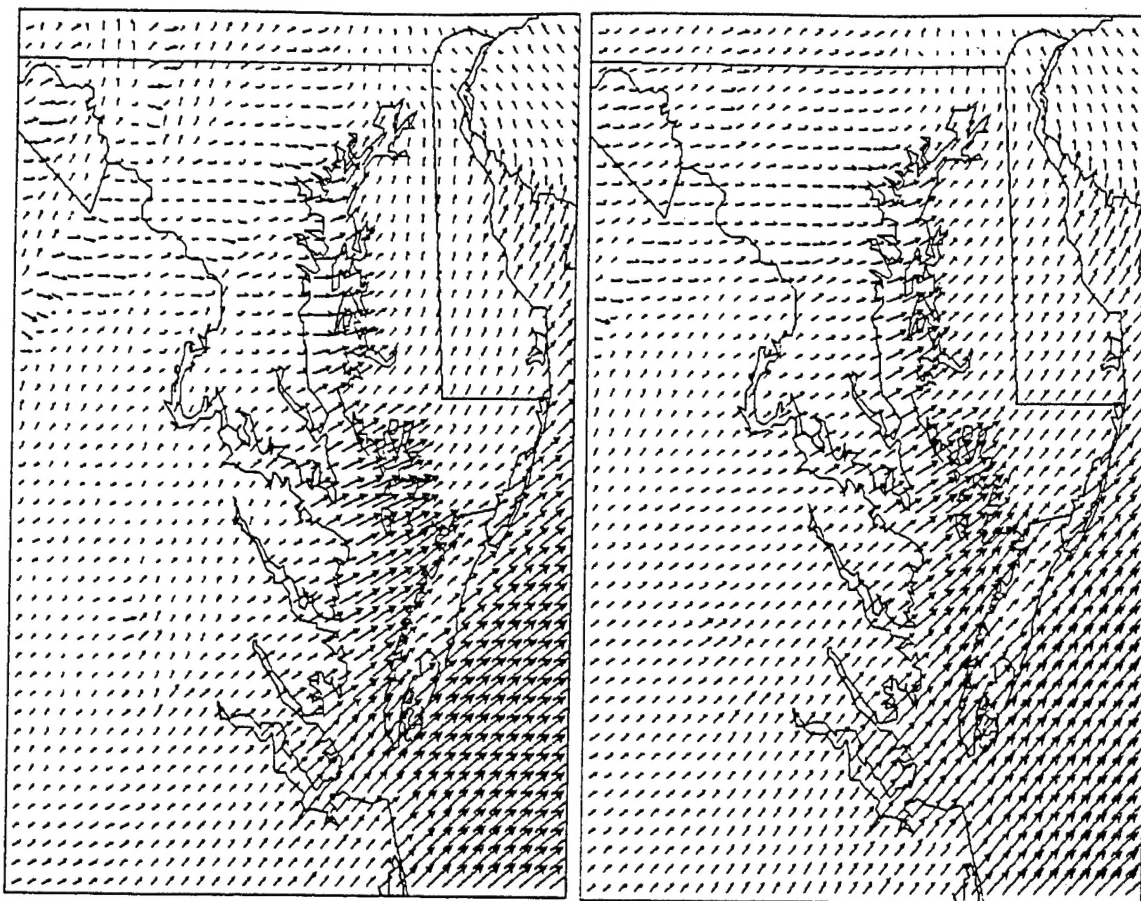


Fig. 3a Surface wind vectors predicted by uncoupled (left) and coupled (right) RAMS for 1100 UTC July 23, 1998. Vectors are drawn every tenth of RAMS finer grids.

Simulation 1: Hours +0 - +14 (1200 - 0200 UTC July 22)

Simulation 2: Hours +12 - +26 (0000 - 1400 UTC July 23)

Simulation 3: Hours +24 - +38 (1200 - 0200 UTC July 23)

Simulation 4: Hours +36 - +50 (0000 - 1400 UTC July 24)

At the beginning of each simulation, RAMS is initialized with ETA's 40 km fields in the east US. The RAMS is run at two different grid resolution: a coarser grid with 16×64 km resolution and a finer grid with 4×4 km grid resolution. The finer grid is nested in the coarser grids which are used to supply the boundary conditions. The coarser grid domain is much larger than the finer grid domain shown in Fig. 1. The RAMS was run twice for 0000, 0100, and 0200 UTC July 23: one for the first simulation and the other to complete a spin-up cycle for the next simulation. These four simulations were completed by repeating the procedure four times.

3.2. The coupled GLERL/RAMS model runs

The coupled GLERL/RAMS model runs started with the GLERL model. It was driven by the first hour uncoupled RAMS wind at 1200 UTC July 22. After z_0 was calculated in the GLERL at every 4 km grid, it was fed back to the RAMS and used as the first hour over water sea surface roughness for RAMS finer grid. Then the RAMS was

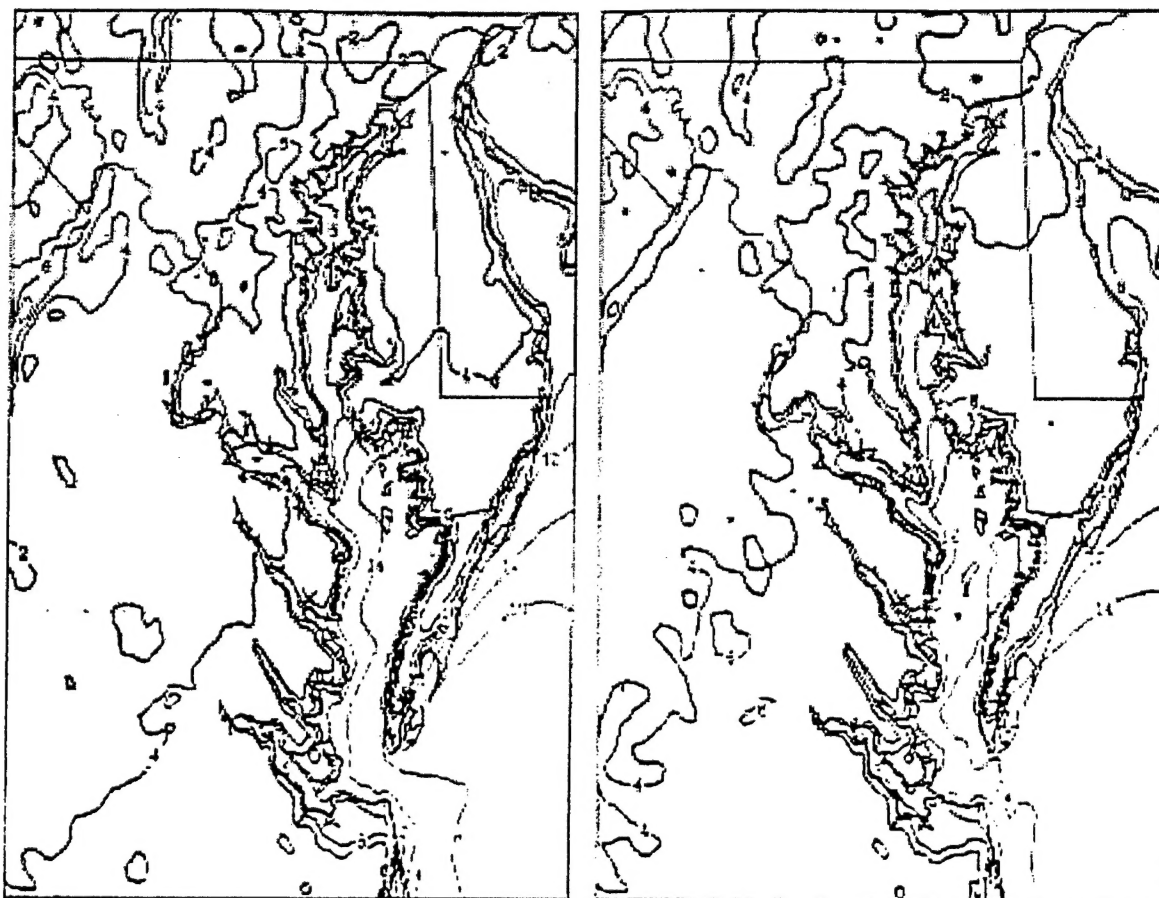


Fig. 3b Surface wind speed contour predicted by uncoupled (left) and coupled (right) RAMS for 1100 UTC July 23, 1998.

initialized with ETA's wind field. The RAMS was run at coarser grid first. The sea surface roughness over the very few water points in the coarser grid were calculated with Eq. (7). The RAMS finer grids used the output from coarser grid as boundary conditions. In RAMS finer grids, z_0 over land changed every time step at 15 s, but z_0 over water was exchanged with the wave model output at each hour. This is justified by the fact that wave condition does not change significantly within an hour period of time and the over water z_0 field can be considered as a constant. For the RAMS predicted 10 m height surface winds, stability was corrected with air and water temperature data from the Chesapeake Bay Observing System (CBOS) (see Fig. 1) and then used to drive the GLERL wave model for the next hour. The process was repeated 14 times to complete a twelve hour simulation.

3.3. Results

The coupled/uncoupled GLERL predicted surface wind waves are compared to the wave data at the tower location. A twenty hour time series model data comparison of significant wave height, H_s , and peak period, T_p , for the coupled and uncoupled model runs is given in Fig. 2. Fig. 2a shows that the significant wave heights predicted by coupled GLERL are in slightly better agreement with data than those predicted by uncoupled model runs. The predicted peak periods by the coupled wave model also show a slightly better agreement with data than those predicted by the uncoupled wave model runs, as shown in Fig. 2b. The large biases for both models at the beginning of the time period are probably due to the RAMS model spin-up.

The difference in H_s and T_p prediction between coupled and uncoupled GLELRL wave model is a result of

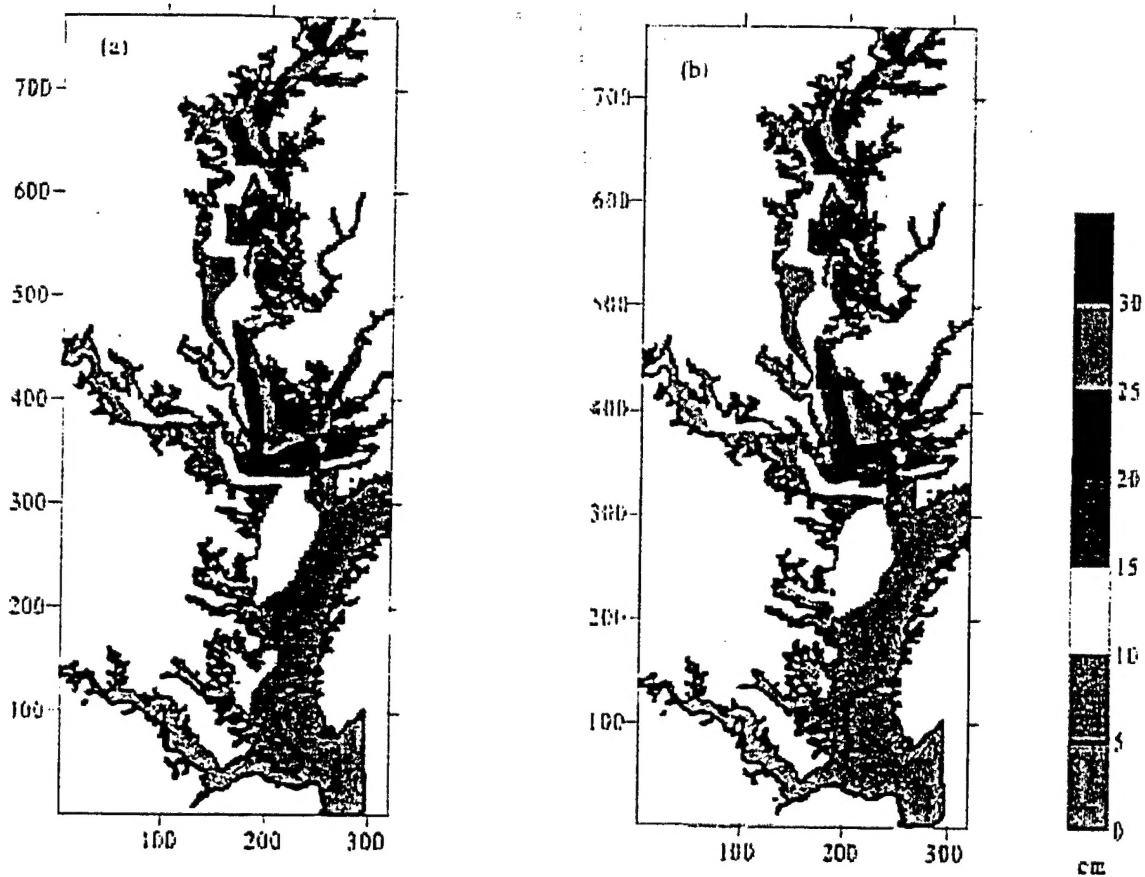


Fig. 4 The significant wave height (cm) field predicted by GLERL wave model. The wind field used is from uncoupled (a) and coupled (b) RAMS model for 1100 UTC July 23, 1998, which is shown in Fig. 3.

the difference between coupled and uncoupled RAMS predicted surface winds (speeds and direction). An example of RAMS predicted surface wind field over the CB for 1100 UTC July 23 is given in Fig. 3a&b for the uncoupled and coupled results. The vector plot in Fig. 3a shows wind direction and speed at every tenth of RAMS finer grids. Both wind vector plot (Fig. 3a) and contour line plot (Fig. 3b) are generated with READY (Realtime Environmental Applications and Display System at <http://www.arl.noaa.gov/ready/cmet.html>), a web based plotting tool developed at ARL/NOAA. Fig. 3 shows that the wind field predicted by coupled RAMS is smoother than the uncoupled wind field over most of the CB. There is a significant difference in the wind speed and direction in the mid-CB area, with wind speed predicted by the coupled RAMS lower than those predicted by the uncoupled RAMS for this hour.

The difference in the wind field predicted by uncoupled and coupled RAMS model results in a significant different wave height (Fig. 4) and peak period field (Fig. 5). Although H_s and T_p predicted by GLERL model with uncoupled and coupled RAMS wind field only show slightly difference at the tower location, there are significant differences for the distributions of H_s and T_p field. Fig. 4 shows that the GLERL predicted wave height is larger in the southern Bay, if the RAMS uncoupled wind field for 1100 UTC July 23 is used. The difference in peak period field for uncoupled (Fig. 5a) and coupled (Fig. 5b) RAMS wind field for the same time is also significant in southern Bay, with a higher T_p prediction by uncoupled wind field.

The sensible heat fluxes predicted by the uncoupled RAMS (Fig. 6a) and coupled RAMS (Fig. 6b) for 1100 UTC July 23 show a significant difference over both land and water in the entire RAMS domain. Sensible heat fluxes

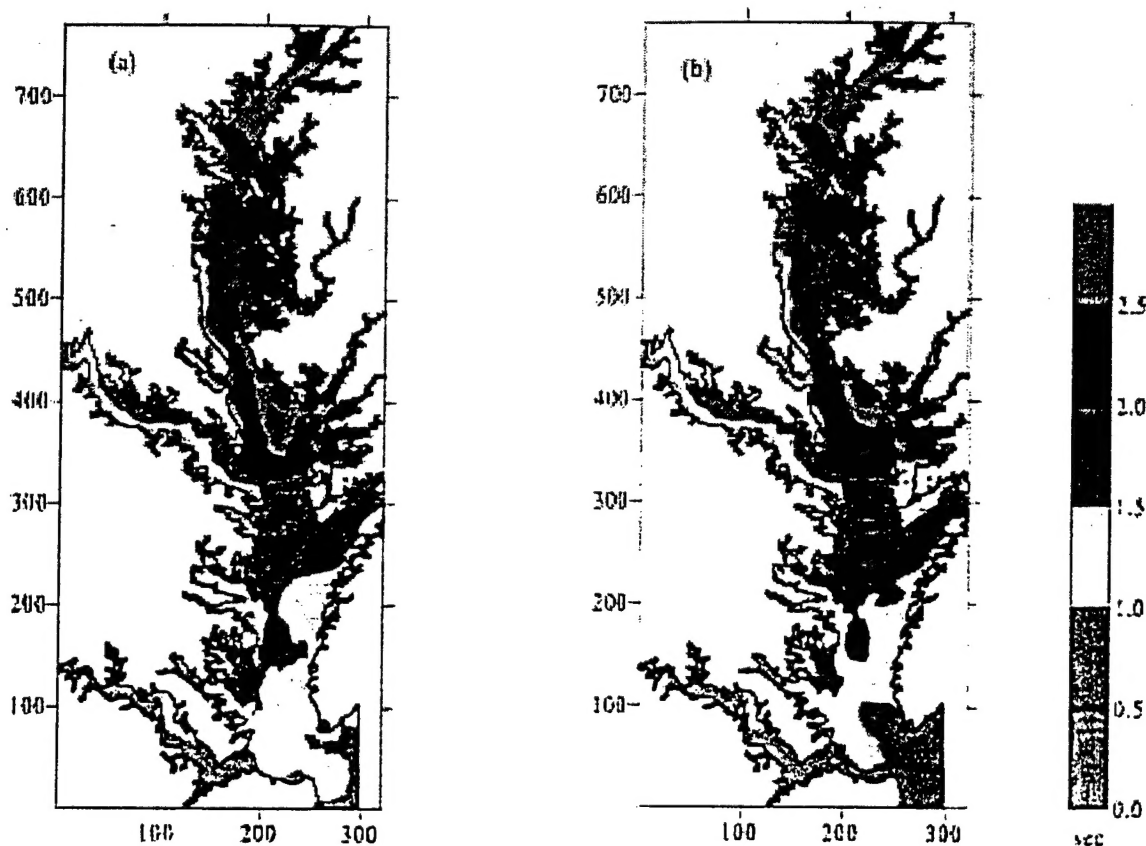


Fig. 5 The peak wave period field (s) predicted by GLERL wave model. The wind field used is from uncoupled (a) and coupled (b) RAMS model for 1100 UTC July 23, 1998, which is shown in Fig. 3.

from the coupled RAMS model in Fig. 6b have more spatial variations over water than the uncoupled model in Fig. 6a.

The latent heat fluxes predicted by the uncoupled RAMS in Fig. 7a is also significantly different from those predicted by the coupled RAMS in Fig. 7b. It is interesting to note that the difference occurs both over land and water, which is similar to the sensible heat fluxes in Fig. 6. Over land, there is a significant difference in both sensible and latent heat fluxes between the coupled and the uncoupled modeling results. Over water, the latent heat fluxes predicted by the coupled model runs in Fig. 7b are smaller than those predicted by uncoupled modeling results in the mid-Bay. However, the latent heat fluxes over the water at the Bay mouth are larger for the coupled model runs in Fig. 7b than those for the uncoupled model runs in Fig. 7a.

The heat fluxes predicted by coupled RAMS are significantly different from those predicted by uncoupled RAMS. This is partly due to the fact that the over water sea surface roughness length in the coupled runs has much more complicated spatial structures than the modified Charnock relationship in Eq. (7) which is previously used in the RAMS model. In the coupled runs, the sea state is a strong function of fetch and varies with the wind speeds and direction. For short fetch, a higher surface roughness is expected for young wind seas; for longer fetch, the surface roughness is relatively lower (Lin et al. 2002). The GLERL predicted sea state dependent sea surface roughness is fed back to the RAMS model during the coupling process. This may account for some of the difference between the coupled and uncoupled results. However, the present study can not explain all the differences between the coupled and uncoupled model runs. One possible explanation is that the RAMS model may be very sensitive to the changing of over water roughness. More coupled model tests are needed to address this issue.

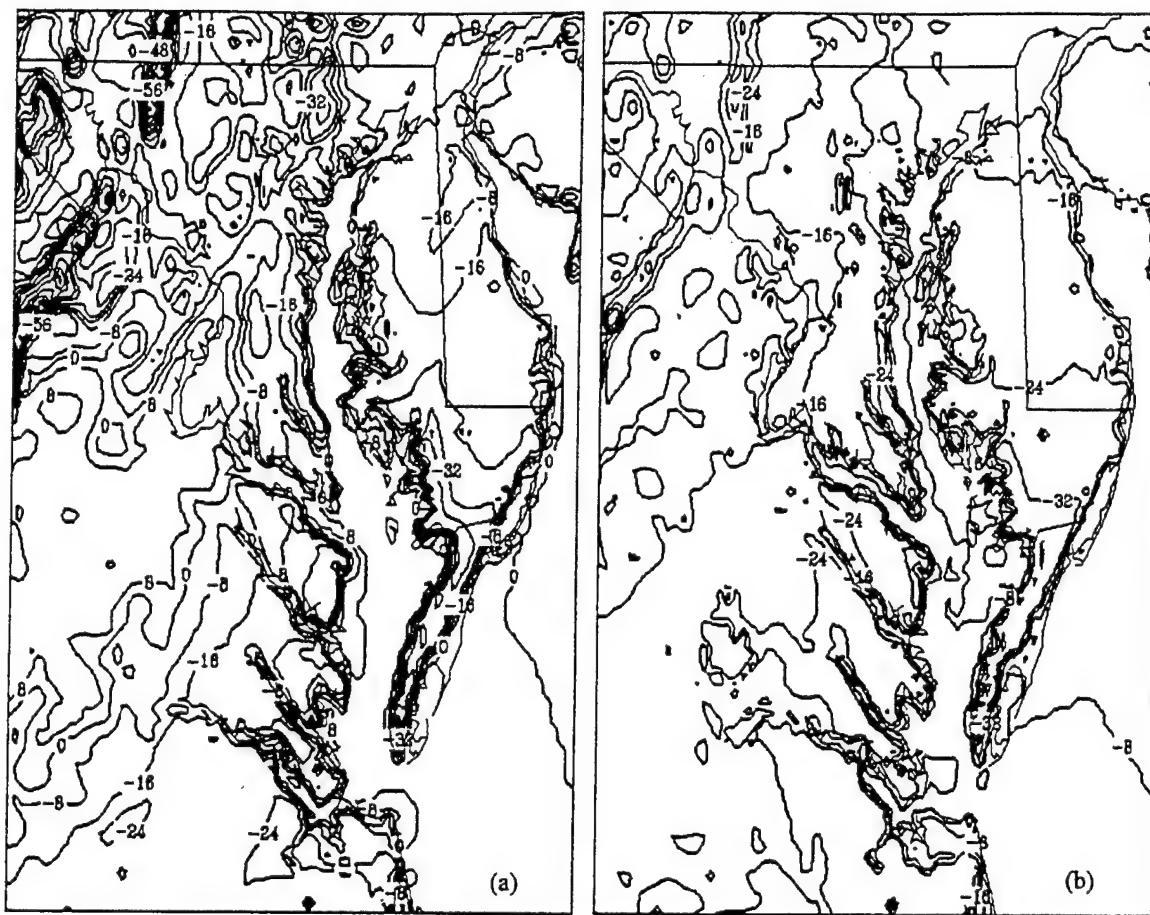


Fig. 6 Sensible heat fluxes predicted by the uncoupled (a) and coupled (b) RAMS model for 1100 UTC July 23, 1998.

4. SUMMARY AND CONCLUSIONS

In this study, surface wind wave effects on air-sea heat and momentum fluxes in the CB is investigated with a fully coupled GLERL/RAMS modeling test against a data set from a tower experiment. Comparisons are made among the coupled and uncoupled modeling results and the tower data. Through this study, it is found that in an entirely fetch limited coastal environment, H_s and T_p predicted by the coupled GLERL agree with the data slightly better than those predicted by the uncoupled model, if compared with data at the tower location. The difference results from the difference between the coupled and uncoupled RAMS wind field. The field distribution of H_s and T_p from coupled and uncoupled GLERL model also shows significant differences in the southern Bay.

Compared with uncoupled RAMS model, the coupled RAMS can predict a significant different wind field (both in wind speed and direction). The coupled model runs tended to give smoother spatial distribution of the wind field than the uncoupled model runs. In the mid-CB, the uncoupled RAMS predicted a higher wind speed than the coupled RAMS, and the wind directions are also different.

The sensible and latent heat fluxes predicted by RAMS model also show a significant difference between the coupled and uncoupled model runs. The difference occurs both over land and water, covering the entire RAMS domain. One obvious reason to account for this difference is the sea state dependent surface roughness that is fed back from

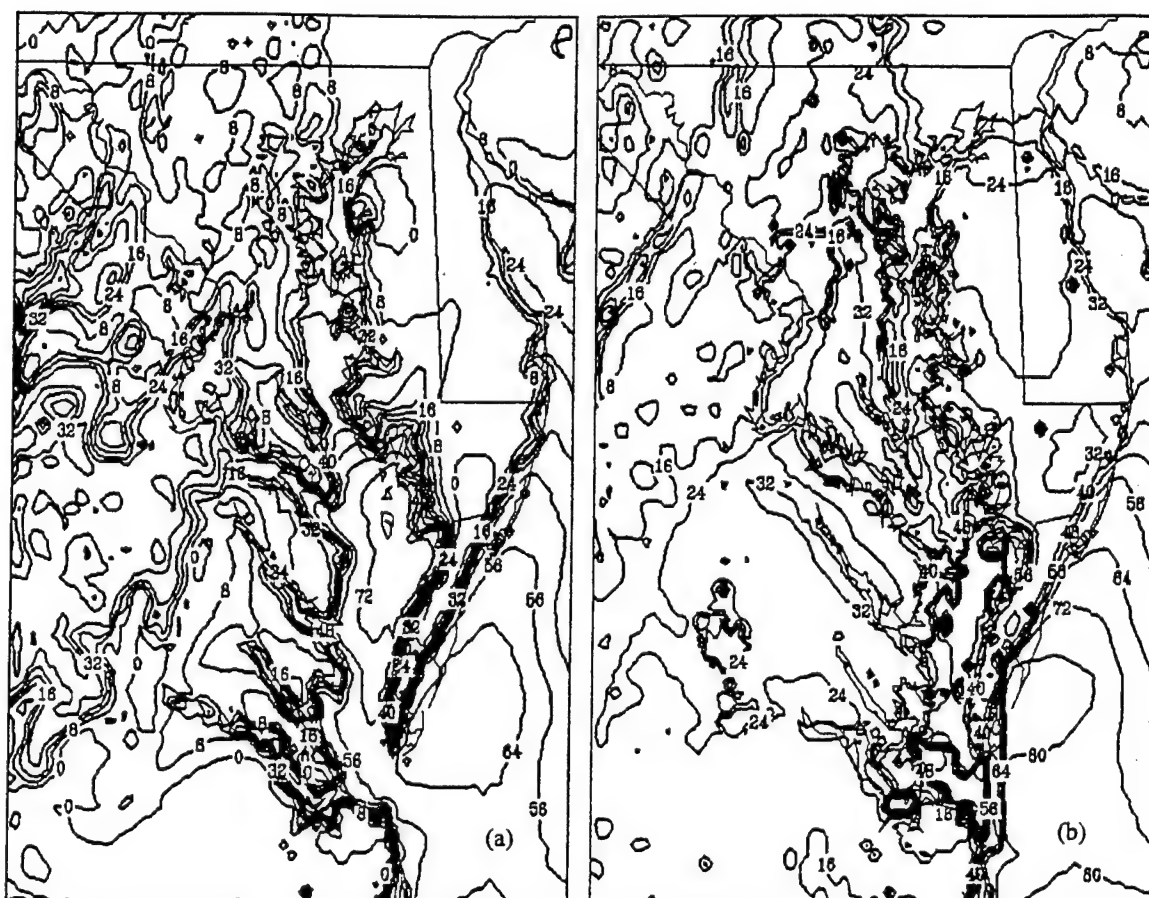


Fig. 7 Latent heat fluxes predicted by the uncoupled (a) and coupled (b) RAMS model for 1100 UTC July 23, 1998.

GLERL to RAMS during the coupling processes. However, the sea state dependent sea surface roughness does not explain all the difference in the heat flux predictions by the RAMS model, which implies that the RAMS model may be quite sensitive to changes in the sea surface roughness parameter.

From this study, we can conclude that the surface wind waves play an important role on the surface winds, sensible and latent heat fluxes in the CB, a fetch limited coastal environment with young wind seas dominate. The significant difference in the surface wind, heat flux prediction between the coupled and uncoupled GLERL/RAMS model shows that it is necessary to develop a coupled modeling system to include sea state dependent surface roughness in the RAMS model. Finally, we would like to point out that the current study does not answer two questions: one is the over water sea surface roughness in low winds; the other is the sensitivity of the RAMS model on the changing sea surface roughness. We would like to pursue more coupled modeling tests in the future to address these issues.

ACKNOWLEDGMENTS

We thank Dr. John Kelly at NOAA/NOS for his help with degribbing the RAMS wind files. We also thank Dr. Frank Aikman at NOAA/NOS for his assistance with computer time. This study was supported by the National Sea Grant Office (Grant No. NA86RG0037) and by the National Ocean Partnership Program (Grant No. N00014-98-1-0837). W. Lin presently hold a CORE/NRL Postdoctoral Fellowship at the Naval Research Laboratory, Stennis Space Center, Mississippi. UMCES Publication No. 3605.

REFERENCES

- Charnock, H., 1955: Wind stress on a water surface. *Quart. J. Roy. Meteor. Soc.*, **81**, 639-640.
- Deane, G. B., and M. D. Stokes, 2002: Scale dependence of bubble creation mechanisms in breaking waves. *Nature*, **418**, 839-844.
- Desjardins, S., J. Mailhot, and R. Lalbeharry, 2000: Examination of the impact of a coupled atmospheric and ocean wave system. Part I: Atmospheric aspects. *J. Phys. Oceanogr.*, **30**, 385-401.
- Donelan, M. A., 1977: A simple numerical model for wave and wind stress prediction. National Water Research Institute Rep., Burlington, ON, Canada, 28 pp.
- Donelan, M. A., 1990: Air-sea interaction. *The Sea*. B. LeMehaute and D. M. Hanes, Eds., Ocean Engineering Science, Vol.9, Wiley and Sons, 239-292.
- Doyle, J. D., 1995: Coupled ocean wave/atmosphere mesoscale model simulations of cyclogenesis. *Tellus*, **47A**, 766-778.
- Geernaert, G. L., S. E. Larsen, and F. Hansen, 1987: Measurements of the wind stress, heat flux, and turbulence intensity during storm conditions over the North Sea. *J. Geophys. Res.*, **92**, 13 127 - 13 139.
- Hasselmann, K., and Coauthors, 1973: Measurement of wind-wave growth and swell decay during the Joint North Sea Wave Project (JONSWAP). *Disch. Hydrogr. Z.*, **12**(Suppl.), A8.
- Janssen, P. A. E. M., 1989: Wave-induced stress and the drag of air flow over sea waves. *J. Phys. Oceanogr.*, **19**, 745-754.
- Janssen, P. A. E. M., 1991: Quasi-linear theory of wind wave generation applied to wave forecasting. *J. Phys. Oceanogr.*, **21**, 1631-1642.
- Lalbeharry, R., J. Mailhot, S. Desjardins, and L. Wilson, 2000: Examination of the impact of a coupled atmospheric and ocean wave system. Part II: Ocean wave aspects. *J. Phys. Oceanogr.*, **30**, 402-415.
- Lin, W., 2000: Modeling surface wind waves and their effects on air-sea fluxes in Chesapeake Bay. Ph.D. dissertation, University of Maryland Center for Environmental Science, Cambridge, MD, 226 pp.
- Lin, W., L. P. Sanford, S. E. Suttles, and R. A. Valigura, 2002: Drag coefficients with fetch limited wind waves. *J. Phys. Oceanogr.*, **32**, (in press).
- Loewen, M. R., 2002: Inside whitecaps. *Nature*, **418**, 830.
- McQueen, J. T., R. R. Draxler, and G. D. Rolph, 1994: Examining the possibility of real-time mesoscale model forecasts in regions of moderately complex terrain. *Proc. 10th Conf. on Numerical Weather Prediction*, Portland, OR, AMS, 412-414.
- McQueen, J. T., R. A. Valigura, and B. J. B. Stunder, 1997: Evaluation of surface flux and turbulence predictions over the Chesapeake Bay from a mesoscale model. *Proc. 13th Conf. on Hydrology*, Long Beach, CA, AMS, 62-65.
- Pielke, R. A., and Coauthors, 1992: A comprehensive meteorological modeling system - RAMS. *Meteor. Atmos. Phys.*, **49**, 69-91.
- Schwab, D. J., J. R. Bennett, P. C. Liu, and M. A. Donelan, 1984: Application of a simple numerical wave prediction model to Lake Erie. *J. Geophys. Res.*, **89**, 3586 - 3592.
- Smith, S. D., and Coauthors, 1992: Sea surface wind stress and drag coefficients: The HEXOS results. *Bound.-Layer Meteor.*, **60**, 109-142.
- Taylor, A. D., 1997: Conformal map transformations for meteorological modelers. *Computers & Geosciences*, **23**, 63-75.
- Valigura, R. A., 1995: Iterative bulk exchange model for estimating air-water transfer of HNO₃. *J. Geophys. Res.*, **100**, 26 045 - 26 050.

PREPRINTS

**7th INTERNATIONAL WORKSHOP ON WAVE
HINDCASTING AND FORECASTING**

**BANFF, ALBERTA
OCTOBER 21-25, 2002**

David Wang NRL USA

Published by:

**Meteorological Service of Canada
Environment Canada
4905 Dufferin Street
M3H 5T4**

Table of Contents

ACKNOWLEDGMENTS	iii
SESSION A: WAVE CLIMATE STUDIES - LARGE SCALE	
A.1 Climatological Assessment of Reanalysis Ocean Data; S. Caires, A. Sterl, J.-R. Bidlot, N. Graham and V. Swail.....	1
A.2 Swell Propagation and Nearshore Wave Climate; Douglas Scott, Donald Resio and Cristobal Pantoja.....	13
A.3 Global-Scale Wave Observations From Voluntary Observing Ships: Assessment of Reliability and Potentialities for Global and Offshore Regions Studies; Sergey K. Gulev, Vika Grigorieva, Andreas Sterl, and David Woolf.....	25
SESSION B: WAVE CLIMATE TREND AND PREDICTION	
B.1 The Wave Climate of the North Atlantic - Past, Present and Future; Val R. Swail, Xiaolan L. Wang and Andrew Cox.....	36
B.2 51-Year Wave Hindcast and Analysis of Wave Height Climate Trend on the Northwestern Pacific Ocean; Masataka Yamaguchi and Yoshio Hatada.....	48
B.3 Intensification of North Pacific Winter Cyclones, 1948-98: Impacts on California Wave Climate; Nicholas E. Graham, R. Rea Strange and Henry F. Diaz.....	60
B.4 A Stochastic Weather Generator to Estimate the Recent and Future Wave Climate at the German North Sea Coast; Arnt Pfizenmayer.....	70
SESSION C: WAVE CLIMATE STUDIES - REGIONAL	
C.1 Wave Climate Study of the Caribbean Sea; M. Calverley, D. Szabo, V. J. Cardone, E.A. Orelup and M. J. Parsons.....	75
C.2 Directional Characteristics of the 1990-1999 Wave Information Studies Gulf of Mexico Hindcast; Barbara A. Tracy.....	87
C.3 A 40-Year High-Resolution Wind and Wave Hindcast for the Southern North Sea; Ralf Weisse, Heinz Günther and Frauke Feser.....	97

C.4 Challenges to Wave Hindcasting in the Caspian Sea; C. Graham, V. J. Cardone, E. A. Ceccacci, M. J. Parsons, C. Cooper and J. Stear.....	105
--	------------

SESSION D: DESIGN WAVE ESTIMATION

D.1 Derivation of a Design Wave from Joint Buoy, Satellite and Hindcast Data Sources; S. VanIseghem	117
D.2 Measured Tropical Cyclone Seas; S. J. Buchan, S. M. Tron and A. J. Lemm	128
D.3 Effects of Distributions and Fitting Techniques on Extreme Value Analysis of Modelled Wave Heights; W. D. Hogg and V. R. Swail	140
D.4 Effects of Sampling Rate on Extreme Value Analysis of Wave Height; Gene Berek	*

SESSION E: WAVE MODELS AND MODEL EVALUATION

E.1 WAM Performance in the Gulf of Mexico with COAMPS Wind; Y. Larry Hsu, W. Erick Rogers and James D. Dykes	151
E.2 SWAN Evaluation in Northern Gulf of Mexico; James D. Dykes, Y. Larry Hsu and W. Erick Rogers	160
E.3 Comparison of the Performances of Three of the State-of-the-Art Ocean Wave Models in Extreme Storm Cases; Roop Lalbeharry	171
E.4 A Fine-Resolution Operational Wave Model System for the NW Atlantic; Bechara Toulany, Will Perrie, Peter C. Smith and Baoshu Yin	182
E.5 The 2002 Release of WAVEWATCH III; Hendrik L. Tolman	188
E.6 Wave-Atmosphere-Ocean Modelling of Recent Storms; W. Perrie, W. Zhang, Z. Long, W. Li and B. Toulany	198
E.7 Coupling GLERL with RAMS to Study Surface Wind Wave Effects on Air-Sea Fluxes in Chesapeake Bay; Weiqi Lin, Lawrence P. Sanford, Jeff McQueen, Steven E. Suttles and Paul A. Hwang	203
E.8 A Method to Predict Wave Conditions in Island Environment; E. Rusu, J. P. Pinto, R. Silva and C. Ventura Soares	215

SESSION F: ROGUE WAVES AND EXTREME CREST HEIGHTS

F.1 Singular Waves, Propagation and Prognosis; H. Günther and W. Rosenthal	227
---	------------

F.2 Investigating Conditions for Rogue Wave Events using a Global Spectral Wave Model; Jim Gunson and Anne Karin Magnussen.....	235#
F.3 Nonlinear Fourier Analysis of Rogue Waves in Random Wave Trains; A. R. Osborne, Donald Resio, Miguel Onorato and Marina Serio	236#
F.4 Wave Focusing on Deep Water - Bandwidth, Spreading and Non-Linearity; Paul H. Taylor and Richard H. Gibbs	237
F.5 The Exceedence Probability of Wave Crests Calculated by the Spectral Response Surface Method; R. Gibson, P. Tromans and C. Swan	249
F.6 Harmonic Distortion in Storm Waves and Consequences for Extreme Crest Heights; M. A. Donelan and A. K. Magnusson	261
F.7 On the Prediction of Extreme Wave Crest Heights; Sverre Haver	270

SESSION G: WAVE THEORY I (Wednesday 8:00 AM)

G.1 A Full-Boltzmann Simulation of Fully Developed Sea Waves; Robert Jensen, Don Resio and Andrei Pushkarev.....	285#
✓ G.2 Theoretical Interpretation of Fetch Limited Wind-Driven Sea Observations; V. E. Zakharov	286
✓ G.3 Direct and Inverse Cascade of Energy, Momentum, and Wave Action in Wind-Driven Sea; S. Badulin, A. Pushkarev, D. Resio and V. Zakharov	295
✓ G.4 The Momentum Flux Balance at the Sea Surface; Donald Resio and Charles Long	307
✓ G.5 A Comparison of the Energy Flux Computation of Shoaling Waves using Hilbert and Wavelet Spectral Analysis Techniques; Paul A. Hwang, James M. Kaihatu and David W. Wang	318

SESSION H: WAVE THEORY II 10:10 AM

✓ H.1 On the Prediction of the Fetch Relations and Dissipation Laws Based on Dual Evolution Equations for Non-Linear , Non-Conservative Wave Systems; Marshall P. Tulin.....	323#
H.2 The Effects of Swell and Wave Steepness on Wave Growth and Depth-Induced Wave Breaking; N. Booij and L. H. Holthuijsen.....	324
H.3 Numerical Simulation of Weak Turbulent Kolmogorov Spectrum in Water Surface Waves; Igor Lavrenov, Don Resio and Vladimir Zakharov	327

	Page
H.4 Using Field Buoy Data to Study Asymmetrical Wave-Wave Interactions in a Horse-Shoe Pattern; Ray-Qing Lin and Lihwa Lin.....	339
 SESSION I: TROPICAL CYCLONE PREDICTION	
I.1 Real-Time Forecasting of Winds, Waves and Surge in Tropical Cyclones; Hans C. Graber	351#
I.2 Variability of Hurricane Wind and Wave Predictions due to Variations in Track and Intensity Projections; Hans C. Graber, Robert E. Jensen, Vincent J. Cardone, Andrew Cox, John L. Guiney, Mark D. Powell and Peter Black.....	352#
 SESSION J: SHALLOW MODEL FORMULATION I	
J.1 On the Analysis of Dispersion Relation of Spatially Shoaling Waves; David W. Wang, James M. Kaihatu and Paul Hwang	353
J.2 Coastal Wave Modelling Validation Using New Field Techniques; Carlos Ventura Soares, Eugen Rusu, Luis Q. Santos, António Pires Silva and Oleg Makarynskyy	361
J.3 Incident Boundary Conditions for Wave Transformation; Jane McKee Smith and Mark B. Gravens	373
J.4 Model Predictions and Sensitivity Analysis of Nearshore Processes over Complex Bathymetry; James M. Kaihatu and William C. O'Reilly	385
J.5 The Impact of Variable Depth and Currents on Wave Development; Heinz Günther, Gerhard Gayer and Wolfgang Rosenthal	397
 SESSION K: SHALLOW MODEL FORMULATION II	
K.1 The Impact of Radiation Stress in a Coupled Wave-Tide-Surge Model; Yin Baoshu, Will Perrie, HouYijun, Lin Xiang and Cheng Minghua	401
K.2 The Application of a Coupled Wind, Water Level and Wave Model in a Warning System Against Flooding; Elizabeth (Ellen) J. Claessens, Johannes (Hans) P. de Waal, Hans C. van Twuiver and Marcel Bottema	410
K.3 Wave Measurements using Upward Looking Sonars in Marginal and Polar Sea Ice Regimes; David Fissel, John Marko and Humfrey Melling.....	422
K.4 Barotropic Waves Generated by Storms Moving Rapidly Over Shallow Water; Doug Mercer, Jinyu Sheng, Richard Greatbatch and Josko Bobanivic	434

SESSION L: OPERATIONAL FORECASTING

L.1 Quantifying the Role of Wind Field Accuracy in the U.S. Navy's Global Ocean Wave Nowcast/Forecast System; W. Erick Rogers and Paul A. Wittmann	437#
L.2 The Distributed Integrated Ocean Prediction System (DIOPS); Dean Wakeham, Richard Allard, John Christiansen, Tom Taxon and Steve Williams	438
L.3 The Effect of Altimeter Sampling Patterns on Estimates of Wave Model Error Correlations; Diana J. M. Greenslade and Ian R. Young	445
L.4 20 Years of Operational Forecasting at Oceanweather; Andrew Cox and Vincent Cardone	458
L.5 A PC-Based Inshore Wave Forecast System; Nigel Tozer and Tyrone Parkinson	471
L.6 Wave Model Validation in the St. Lawrence River Estuary; Denis Jacob, Will Perrie, Bechara Toulany, François Saucier, Denis Lefavre and Viateur Turcotte.....	477

POSTERS

P.1 Upper Limit on Wave Height in Dynamic Fetch; Ralph Bigio	484
P.2 North Atlantic Wave Climate Extremes and their Variability; E. A. Orelup, A. Niitsoo and V. J. Cardone.....	490
P.3 Case Studies of Tropical to Extra-Tropical Cyclone Conversion in the Western North Atlantic: Wind Field Kinematics and Wave Response; Andrew T. Cox, Brian T. Callahan, Vincent J. Cardone and Val R. Swail	493
P.4 Focused Waves onto a Plane Beach; A. C. Hunt, P. H. Taylor, A. G. L. Borthwick, P. K. Stansby and T. Feng.....	*
P.5 The Partition of Energy into Waves and Currents; W. Perrie, C. Tang, Y. Hu and B. M. DeTracy	498
P.6 Impact of Bottom Stress and Currents on Wave-Current Interactions; Yin Baoshu, Will Perrie, HouYijun, Lin Xiang and Cheng Minghua	504
P.7 Artificial Neural Networks in the Forecasting of Wave Parameters; Oleg Makarynskyy, António A. Pires-Silva, Dina Makarynska and Carlos Ventura-Soares	514
P.8 Methods to Reduce Biases in Wind Speeds from Ships and Buoys; Bridget Thomas and Val Swail	523